Journal of Power Sources 222 (2013) 373–378

Contents lists available at SciVerse ScienceDirect

Journal of Power Sources

journal homepage: www.elsevier.com/locate/jpowsour

Improving electrochemical performance of $Li_3V_2(PO_4)_3$ in a thiophene-containing electrolyte

Meng Hu, Jinping Wei*, Liying Xing, Zhen Zhou*

Key Laboratory of Advanced Energy Materials Chemistry (Ministry of Education), Institute of New Energy Material Chemistry, Nankai University, Tianjin 300071, China

HIGHLIGHTS

- ► *In situ* electropolymerization of thiophene in the conventional organic electrolyte improved $Li_3V_2(PO_4)_3$ cathode materials.
- ► The cathode materials exhibited higher reversible capacity and better rate performance.
- ► The addition of thiophene improved the deintercalation/intercalation of the third Li^+ ion at high electrode potentials.

GRAPHICAL ABSTRACT

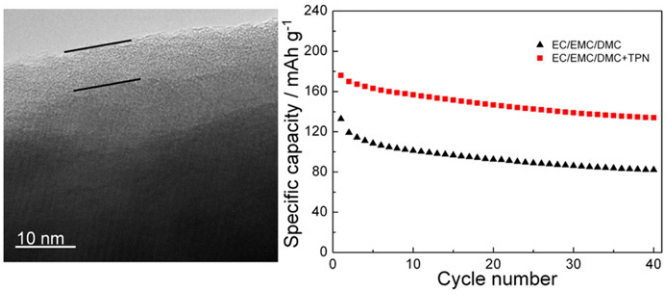

ARTICLE INFO

Article history:
Received 6 March 2012
Received in revised form
2 September 2012
Accepted 3 September 2012
Available online 10 September 2012

Keywords:
$Li_3V_2(PO_4)_3$
Li ion batteries
Electrolytes
Thiophene
Coating

ABSTRACT

In order to inhibit the decomposition of the electrolytes and improve the performance of $Li_3V_2(PO_4)_3$ cathode materials at high potentials, we propose a conducting polymer coating method by the *in situ* electropolymerization of thiophene which was added to conventional organic electrolytes. The formation of polythiophene film on $Li_3V_2(PO_4)_3$ surface was demonstrated by high-resolution transmission electron microscopy and X-ray photoelectron spectroscopy. Polythiophene-coated $Li_3V_2(PO_4)_3$ cathode materials exhibited higher reversible charge/discharge capacity and better rate performance. Electrochemical impedance spectroscopy indicated that the addition of thiophene decreased the decomposition of the electrolytes on the cathode surface and improved the electronic conductivity of $Li_3V_2(PO_4)_3$, allowing Li^+ ions in $Li_3V_2(PO_4)_3$ to deintercalate/intercalate more smoothly.

© 2012 Elsevier B.V. All rights reserved.

1. Introduction

Though Li ion batteries are the most popular portable power source in the current society, their energy and power density cannot satisfy the requirement for the applications in electric vehicles (EVs) and hybrid EVs (HEVs) [1–4]. For this purpose, developing cathode materials with large capacities and high voltages is urgent. Recently, extensive investigations have been taken on the monoclinic $Li_3V_2(PO_4)_3$ [5–21], which can extract/insert two Li^+ ions when cycled between 3.0 V and 4.3 V, and when charged to 4.8 V, the third Li^+ ion can be extracted, exhibiting a theoretical capacity of 197 mAh g^{-1}, and average discharge voltage of 3.8 V [5,14,15]. Thus, $Li_3V_2(PO_4)_3$ can achieve higher energy density than $LiCoO_2$ and $LiFePO_4$.

However, when charged to 4.8 V, $Li_3V_2(PO_4)_3$ encounters severe problems: conventional electrolytes composed of $LiPF_6$ and organic carbonate solvents are oxidized above 4.5 V [22]. Moreover, transition-metal cations can catalyze the oxidation reaction and

* Corresponding authors. Tel.: +86 22 23503623; fax: +86 22 23498941.
E-mail addresses: jpwei@nankai.edu.cn (J.P. Wei), zhouzhen@nankai.edu.cn (Z. Zhou).

0378-7753/$ – see front matter © 2012 Elsevier B.V. All rights reserved.
http://dx.doi.org/10.1016/j.jpowsour.2012.09.005

accelerate the decomposition of electrolytes [23,24]. In addition, the complete extraction of three Li^+ ions will lead to serious structural transformation [16]. Actually, the third Li^+ cannot be extracted smoothly at high potentials, leading to poor charge capacity and cyclability. Accordingly, most previous reports were based on the extraction/insertion of two Li^+ ions (charged to 4.3 V), which could not exert the potential of high capacity and high energy density in $Li_3V_2(PO_4)_3$. For the purpose of improving the behaviour of $Li_3V_2(PO_4)_3$ at high potentials, two strategies should be considered: the inhibition of electrolyte decomposition and the improvement of intrinsic electrochemistry of $Li_3V_2(PO_4)_3$. This work mainly focused on the inhibition of the electrolyte decomposition.

Surface coating could prevent the direct contact of the electrolytes and the cathode surface, and then the decomposition of the electrolytes eletrocatalyzed by transition metals will be decreased. Carbon coating proves an effective way for such purpose in polyoxyanionic materials [25–30]. However, the additional excessive carbon coating would increase the production cost and decrease the tap density of active materials. It has been reported that conducting polymers can improve the performance of $LiCoO_2$ [31], $LiFePO_4$ [32,33], and other cathode materials [34,35]; several coating methods have been employed, including electrochemical deposition on cathode particles [36], chemical oxidative polymerization [37], and microwave-solvothermal approach [38]. Apparently, the synthetic routes are complicated and difficult for large-scale production.

Here we propose a simple and effective method to coat $Li_3V_2(PO_4)_3$ with conducting polymers by adding appropriate amount of thiophene (TPN) to conventional organic electrolytes. Thiophene can be electrochemically polymerized to polythiophene (PTh) [39,40] at the potential of ~4.4 V vs. Li/Li^+ [41], which is lower than the decomposition potential of the electrolyte compositions. Also, it has been reported that vinylene carbonate (VC) could be polymerized at high potentials on the cathode surface, and the performance of the cathodes was accordingly improved by decreasing the decomposition of electrolytes [42,43]. However, the formation of PTh film can not only suppress the decomposition of electrolytes, but also improve the electrical conductivity of $Li_3V_2(PO_4)_3$ significantly, since PTh possesses conjugated π network and demonstrates excellent electrical conductivity for $Li_3V_2(PO_4)_3$ cathodes.

2. Experimental

2.1. Material preparation

$Li_3V_2(PO_4)_3$ was synthesized by adopting V_2O_5, oxalic acid, Li_2CO_3 and $NH_4H_2PO_4$ as starting materials. A stoichiometric mixture of V_2O_5 and oxalic acid was dissolved in deionized water with magnetic agitation at 70 °C. Li_2CO_3 and $NH_4H_2PO_4$ in the stoichiometric ratio were added to the solution and stirred at 70 °C to remove the excess water. After a blue gel formed, the gel precursor was dried at 100 °C in air. The precursor was heated at 350 °C for 4 h in flowing argon. The mixture was ground, pressed into pellets and heated at 750 °C for 4 h in flowing argon.

2.2. Material characterization

The phase of the sample was confirmed with X-ray diffraction (XRD, D/MAX III diffractometer with Cu Kα radiation). Surface analysis of the cathodes was taken after the cells completed 40 charge/discharge cycles. The cathode films of the cells were taken out and washed with anhydrous ethanol for three times and dried at 100 °C for 24 h in vacuum to remove the residual electrolytes. The morphology of the cathodes was characterized by high-resolution transmission electron microscope (HRTEM, FEI Tecnai G2 F20). The content of carbon was determined with thermogravimetry and differential thermal analysis (TG–DTA, Rigaku PTC-10A). Surface element analysis was performed by X-ray photoelectron spectroscopy (XPS, Axis Ultra DLD, Kratos Analytical Ltd.).

2.3. Preparation of electrolytes

The standard electrolyte was 1 M $LiPF_6$ dissolved in a mixture of ethylene carbonate (EC), ethyl methyl carbonate (EMC) and dimethyl carbonate (DMC) (1:1:1 by volume). The optimized electrolyte was prepared by mixing the standard electrolyte with 0.1 wt.% thiophene and stirring for 24 h in an argon-filled glove box.

2.4. Electrochemical tests

The electrochemical window of the electrolytes was measured by linear sweep voltammetry (LSV) at a scan rate of 1 mV s^{-1} in a three-electrode system with a platinum foil as the working electrode, and two lithium foils as counter and reference electrodes on a CHI600 electrochemical analyzer (Shanghai Chenhua, China). The $Li_3V_2(PO_4)_3$ electrodes were prepared with $Li_3V_2(PO_4)_3$, acetylene black, and polytetrafluoroethylene (PTFE) binder with a weight ratio of 85:10:5. Test cells of $Li_3V_2(PO_4)_3$/electrolyte/lithium with different electrolytes were assembled in an argon-filled glove box. Galvanostatic charge/discharge tests were performed on a Land CT2001 battery tester between 3.0 and 4.8 V at room temperature. Cyclic voltammograms (CVs) were performed on a Zahner-Elektrik IM6e electrochemical workstation in a potential range of 3.0–4.9 V at a scan rate of 0.1 mV s^{-1}. Electrochemical impedance spectroscopy (EIS) was also recorded on the electrochemical workstation with the frequency ranging from 100 kHz to 10 mHz.

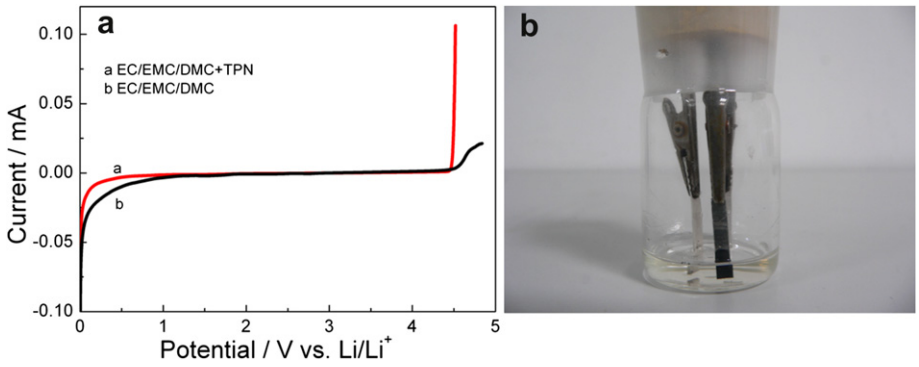

Fig. 1. LSV curves of the electrolytes with or without thiophene (a) and the image of the electrode in the electrolyte with thiophene after the LSV test (b).

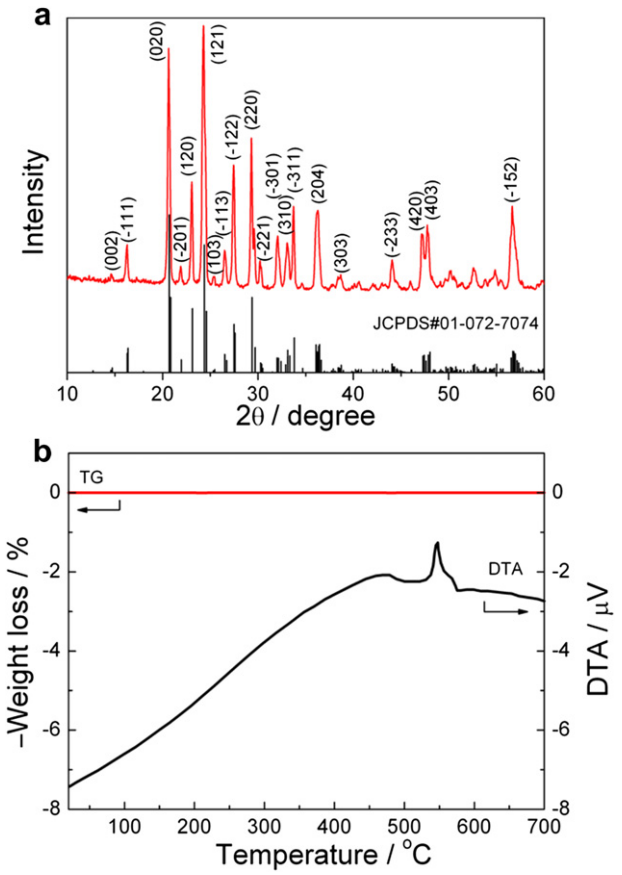

Fig. 2. XRD patterns (a) and TG–DTA curves (b) of $Li_3V_2(PO_4)_3$.

3. Results and discussion

The electrolytes showed different electrochemical behaviours due to the addition of thiophene. As disclosed by the LSV curves in a three-electrode system (Fig. 1(a)), the standard electrolyte is oxidized at 4.5 V vs. Li/Li^+. After the addition of 0.1 wt.% thiophene, the anodic limiting current is observed at 4.4 V, corresponding to the electrochemical polymerization of thiophene. From the picture of the three-electrode system in the thiophene-containing electrolyte after the LSV test (Fig. 1(b)), we can see that a black film was deposited on the platinum working electrode, which is consistent with the previous reports [44,45].

$Li_3V_2(PO_4)_3$ was prepared through a conventional route [9], and the XRD patterns are shown in Fig. 2(a). All the diffraction peaks are indexed as a monoclinic $Li_3V_2(PO_4)_3$ phase with the space group of $P2_1/n$ (JCPDS#01-072-7074). There is no residual carbon in the final $Li_3V_2(PO_4)_3$ sample according to the TG/DTA curves (see Fig. 2(b)). The $Li_3V_2(PO_4)_3$ cathodes were tested in the electrolytes with and without thiophene addition. The HRTEM images of the cycled cathodes are shown in Fig. 3. The surface of the cycled cathodes in the standard electrolyte has irregular interphase film of ~1 nm due to the decomposition of the electrolyte, which is not thick enough to prevent the contact of the electrolyte and the cathode surface. While a uniform coating film of about 5–8 nm is observed on the surface of the cathodes cycled in the thiophene-containing electrolyte.

The XPS results of the fresh and cycled cathode films in the electrolytes with or without thiophene are shown in Fig. 4. According to the C_{1s} spectra, two peaks at 292.4 eV (C–F) and 284.8 eV (C–C) are observed from the fresh cathodes, which belong to PTFE and acetylene black, respectively. After cycling in the standard electrolyte, two new peaks (290 eV for C=O and 286 eV for C–O) appear due to the interphase film, which is generated from the decomposition of carbonate electrolytes on the cathode surface. A peak for C–S bonds at 287.8 eV is observed on the cathodes cycled in the thiophene-containing electrolyte, indicating the presence of PTh on the surface of $Li_3V_2(PO_4)_3$ cathodes. A single peak for PTFE (689.6 eV) is observed from the F_{1s} spectra of all the samples. The peak of LiF (688 eV) is due to the decomposition of the electrolyte. From the S_{2p} spectra, only the cathodes cycled in the thiophene-containing electrolyte possess a peak at 164.8 eV (C–S), which is in agreement with the C_{1s} spectra. From the surface concentration of the elements (Table 1), we can see that the cycled cathodes both have lower F and V content because of the surface film on the cathode surface. Moreover, due to the generation of PTh film on the surface, the cathodes cycled in the thiophene-containing electrolyte have the lowest content of F and V. In addition, the S content is consistent with the S_{2p} spectra (Fig. 4), sufficiently demonstrating the presence of PTh film.

In the thiophene-containing electrolyte, the electrochemical performance of $Li_3V_2(PO_4)_3$ was significantly improved, disclosed by various electrochemical measurements. The initial galvanostatic discharge/charge curves of $Li/Li_3V_2(PO_4)_3$ test cells with different electrolytes are shown in Fig. 5(a), at a current density of 0.1 C (19.7 mA g^{-1}). The four charge plateaus around 3.6, 3.7, 4.1 and 4.5 V correspond to the deintercalation of 0.5, 1, 2, and 3 Li^+, respectively. Three discharge plateaus around 4.0, 3.6 and 3.5 V are clearly observed in the differential capacity dQ/dV (Q, capacity; V,

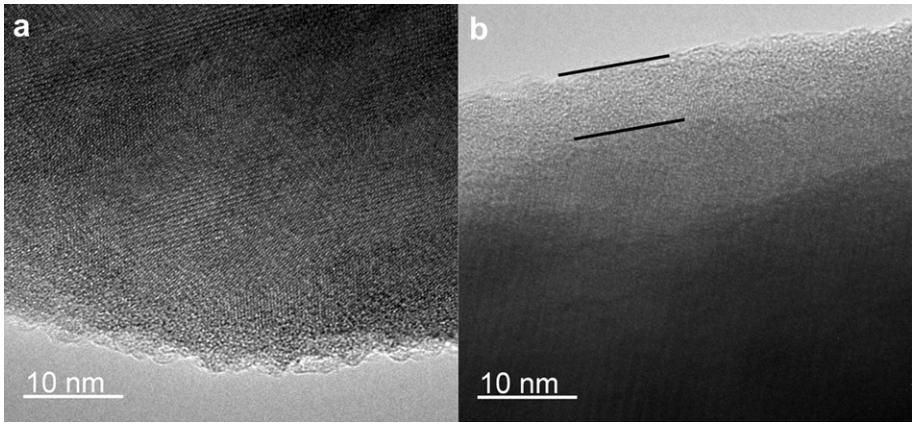

Fig. 3. HRTEM images of the cycled cathodes in the electrolyte without (a), or with (b) thiophene.

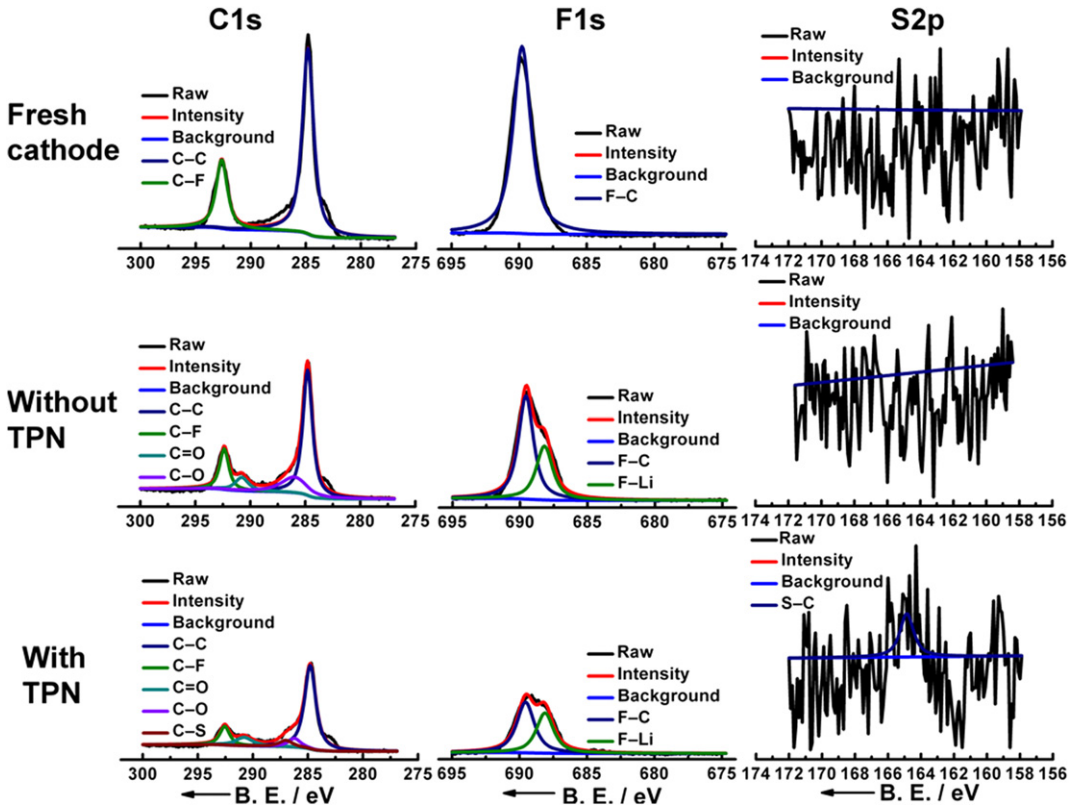

Fig. 4. XPS analysis of fresh and cycled cathodes in the electrolyte with or without thiophene.

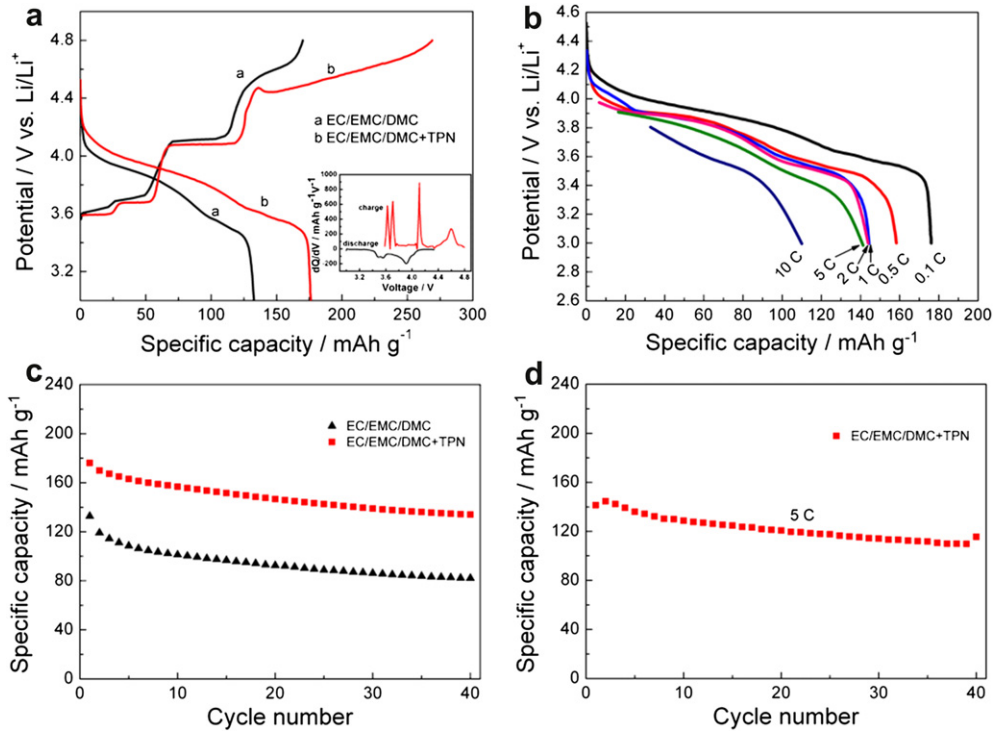

Fig. 5. Initial galvanostatic discharge/charge curves of Li/$Li_3V_2(PO_4)_3$ test cells with different electrolytes. Inset is the differential capacity dQ/dV plot (a). Discharge curves of $Li_3V_2(PO_4)_3$ in the thiophene-containing electrolytes at different rates (b). Cyclic performance of $Li_3V_2(PO_4)_3$ cathodes in the different electrolytes at 0.1 C (c). Cyclic performance of $Li_3V_2(PO_4)_3$ cathodes in the thiophene-containing electrolyte at 5 C (d).

Table 1
Surface concentration (wt.%) of the elements in $Li_3V_2(PO_4)_3$ cathode films.

	C	O	F	P	V	S
Fresh cathode	35.04	21.31	29.27	7.69	6.69	0.00
Without TPN	34.80	23.45	27.33	8.52	5.90	0.00
With TPN	29.82	32.48	20.96	11.91	4.55	0.27

Table 2
Potential differences between the anodic and cathodic peaks of $Li_3V_2(PO_4)_3$ with different electrolytes.

	$E_{O1} - E_{R1}$ (V)	$E_{O2} - E_{R2}$ (V)	$E_{O3} - E_{R3}$ (V)
EC/EMC/DMC	0.172	0.632	0.890
EC/EMC/DMC + TPN	0.149	0.601	0.825

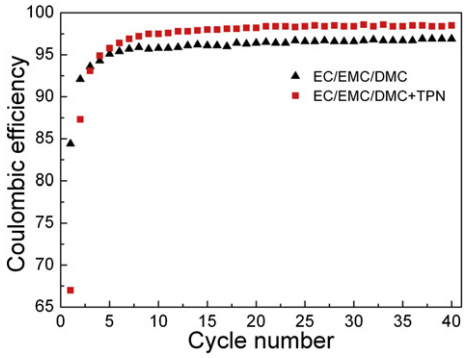

Fig. 6. Coulombic efficiency of $Li_3V_2(PO_4)_3$ cathodes in the different electrolytes at 0.1 C.

voltage) plots (see the inset of Fig. 5(a)). Compared with the standard electrolyte, the cells with the electrolyte containing 0.1 wt.% thiophene presented almost the same charge capacity (~130 mAh g^{-1}) below 4.4 V, which approaches the theoretical capacity of the deintercalation of two Li^+ ions in $Li_3V_2(PO_4)_3$ (133 mAh g^{-1}). However, the charge capacity at the charge plateau around 4.5 V is discriminative. After the addition of thiophene, the charge capacity exceeds the theoretical capacity of deintercalating three Li^+ ions in $Li_3V_2(PO_4)_3$ (197 mAh g^{-1}), which is mainly attributed to the electrochemical polymerization of thiophene. The higher discharge capacity indicates that more Li^+ ions are involved in the electrochemical reactions of the cathode material. The voltage drop between charge and discharge profiles also decreases obviously in the cells with the thiophene-containing electrolyte, indicating the decrease of polarization.

The discharge capacities of $Li_3V_2(PO_4)_3$ in the electrolytes with or without thiophene are 176.1 and 132.8 mAh g^{-1}, respectively. When the rates are 0.5 C, 1 C, 2 C, and 5 C (Fig. 5(b)), the first discharge capacities are 158.3, 144.4, 143.9, and 141.3 mAh g^{-1}, respectively. Even at the high rate of 10 C, the capacity can still reach 110 mAh g^{-1}. After 40 cycles at 0.1 C, the discharge capacity is 134 and 82.1 mAh g^{-1}, respectively (Fig. 5(c)). When cycled at 5 C in the thiophene-containing electrolyte, the capacity retention is 81.7% after 40 cycles (Fig. 5(d)), demonstrating excellent cyclic stability. Low coulombic efficiencies of the initial three cycles in the cells with thiophene addition result from the irreversible electrochemical polymerization of thiophene (Fig. 6). After the initial cycles, the coulombic efficiencies increase to 98.5%. The PTh film reduces the decomposition of electrolyte on the surface of $Li_3V_2(PO_4)_3$ cathodes. Moreover, the PTh film increases the electrical conductivity of $Li_3V_2(PO_4)_3$ cathodes, and decreases the ohmic polarization. Therefore, PTh-coated $Li_3V_2(PO_4)_3$ cathodes demonstrate higher discharge capacity and better cyclability.

From the CV curves in Fig. 7(a), four anodic peaks and three cathodic peaks are observed, although the two cathodic peaks around 3.5 V are difficult to be distinguished because of the structural characteristics of $Li_3V_2(PO_4)_3$. After the coating of PTh, higher peak current density appears, indicating higher electrochemical reaction activity of the cathodes. The peak of the electropolymerization of thiophene is overlapped with the peak of the deintercalation of the third Li^+ (start at ~4.4 V). The potential differences between the anodic and the corresponding cathodic peaks are compared in Table 2. The smaller potential differences demonstrate the better electrochemical reversibility due to the PTh coating. Fig. 7(b) shows the CV curves of $Li_3V_2(PO_4)_3$ electrodes in the electrolyte with thiophene for the initial 3 cycles. The potential differences decrease after the first cycle and remain stable.

Fig. 8 shows the Nyquist plots of $Li_3V_2(PO_4)_3$ electrodes cycled in different electrolytes and measured before cycling and after 40 cycles. In a Nyquist plot, the semicircle in high frequency corresponds to the resistance of the interphase film, the semicircle in medium frequency represents the charge transfer impedance, and the inclined line in the low frequency is attributed to the diffusion of Li^+. Before the first cycle, both the cells exhibit similar size of semicircle, illustrating similar charge transfer impedance. However, after 40 cycles, the semicircles in high frequency are emerged, illustrating the generation of the interphase film on $Li_3V_2(PO_4)_3$ cathodes. Compared with the pure $Li_3V_2(PO_4)_3$ cathodes, the PTh-coated $Li_3V_2(PO_4)_3$ cathodes show lower charge transfer impedance and interphase resistance. The EIS results indicate that the PTh film not only prevents the excessive oxidative decomposition of the electrolyte composition on the cathode surface, decreasing the impedance of interphase films, but also improves the electrical conductivity of $Li_3V_2(PO_4)_3$ cathodes and decreases the charge transfer impedance.

Note that the phase transition and low ion diffusion of $Li_3V_2(PO_4)_3$ are other major reasons for its poor electrochemical

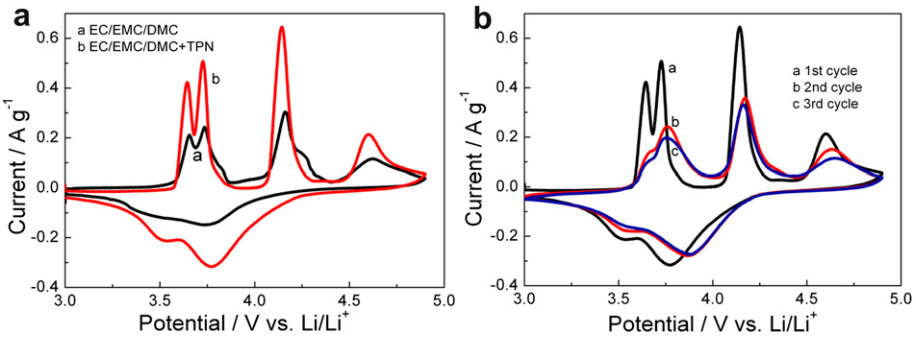

Fig. 7. CV curves of $Li_3V_2(PO_4)_3$ in different electrolytes (a). CV curves of $Li_3V_2(PO_4)_3$ electrodes in the thiophene-containing electrolyte for the initial 3 cycles (b).

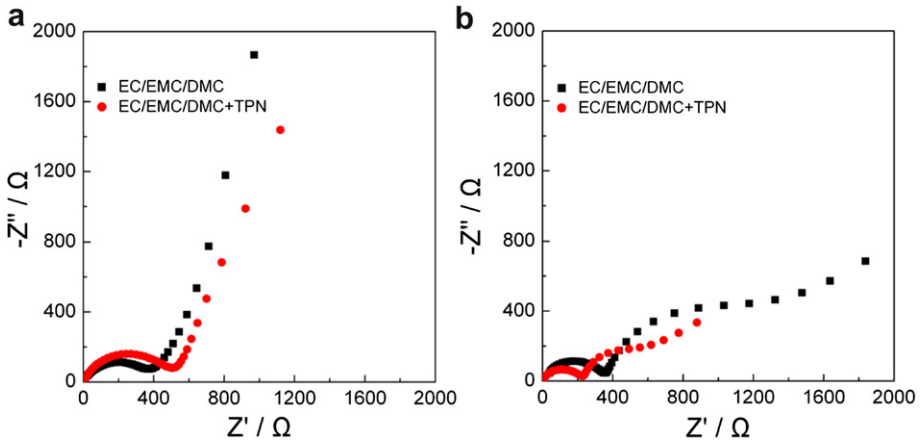

Fig. 8. Nyquist plots of $Li_3V_2(PO_4)_3$ electrodes cycled in different electrolytes and measured before cycling (a) and after 40 cycles (b) at the potential of 3.0 V.

performance at high potentials. In this work, we only considered to inhibit the decomposition of the electrolytes on the cathode surface at high potentials; naturally, efforts are also necessary to improve the intrinsic electrochemistry of $Li_3V_2(PO_4)_3$ to maximize its potentials as high-voltage cathode materials for Li ion batteries.

4. Conclusion

In summary, in order to decrease the decomposition of the electrolytes and improve the performance of $Li_3V_2(PO_4)_3$ cathode materials at high potentials, we proposed a simple and effective method of adopting thiophene-containing electrolytes. Thiophene can be *in situ* electrochemically polymerized into PTh film to passivate the cathode surface, and to decrease the catalytic decomposition of the electrolytes. Moreover, the PTh film improved the electrical conductivity of $Li_3V_2(PO_4)_3$, and decreased the ohmic polarization. Therefore, more Li^+ ions in $Li_3V_2(PO_4)_3$ could deintercalate/intercalate with less side reactions at high potentials, resulting in higher reversible charge/discharge capacities, better rate performance, and longer cyclability. This method is cheap and easy for industrial production and can also be employed to other high-voltage cathode materials. Besides, the coating process is performed after the synthesis of cathode materials; therefore, lower tap density by the excessive coating of carbon or other materials can be avoided, and higher energy density can be expected compared with other coating methods.

Acknowledgements

This work was supported by the 973 Program (2009CB220100) and the Fundamental Research Funds for the Central Universities in China.

References

[1] M. Armand, J.M. Tarascon, Nature 451 (2008) 652.
[2] R. Marom, S.F. Amalraj, N. Leifer, D. Jacob, D. Aurbach, J. Mater. Chem. 21 (2011) 9938.
[3] L.W. Su, Y. Jing, Z. Zhou, Nanoscale 3 (2011) 3967.
[4] G. Jeong, Y.U. Kim, H. Kim, Y.J. Kim, H.J. Sohn, Energy Environ. Sci. 4 (2011) 1986.
[5] H. Huang, S.C. Yin, T. Kerr, N. Taylor, L.F. Nazar, Adv. Mater. 14 (2002) 1525.
[6] P. Fu, Y.M. Zhao, Y.Z. Dong, X.N. An, G.P. Shen, J. Power Sources 162 (2006) 651.
[7] J. Barker, R.K.B. Gover, P. Burns, A. Bryan, J. Electrochem. Soc. 154 (2007) A307.
[8] L.S. Cahill, R.P. Chapman, J.F. Britten, G.R. Goward, J. Phys. Chem. B 110 (2006) 7171.
[9] M.M. Ren, Z. Zhou, X.P. Gao, W.X. Peng, J.P. Wei, J. Phys. Chem. C 112 (2008) 5689.
[10] L.S. Cahill, C.W. Kirby, G.R. Goward, J. Phys. Chem. C 112 (2008) 2215.
[11] M. Morcrette, J.B. Leriche, S. Patoux, C. Wurm, C. Masquelier, Electrochem. Solid-State Lett. 6 (2003) A80.
[12] S. Patoux, C. Wurm, M. Morcrette, G. Rousse, C. Masquelier, J. Power Sources 119 (2003) 278.
[13] C. Deng, S. Zhang, S.Y. Yang, Y. Gao, B. Wu, L. Ma, B.L. Fu, Q. Wu, F.L. Liu, J. Phys. Chem. C 115 (2011) 15048.
[14] M.Y. Saidi, J. Barker, H. Huang, J.L. Swoyer, G. Adamson, Electrochem. Solid-State Lett. 5 (2002) A149.
[15] M.Y. Saidi, J. Barker, H. Huang, J.L. Swoyer, G. Adamson, J. Power Sources 119 (2003) 266.
[16] S.C. Yin, H. Grondey, P. Strobel, M. Anne, L.F. Nazar, J. Am. Chem. Soc. 125 (2003) 10402.
[17] S.C. Yin, H. Grondey, P. Strobel, H. Huang, L.F. Nazar, J. Am. Chem. Soc. 125 (2003) 326.
[18] Y.Q. Qiao, X.L. Wang, Y. Zhou, J.Y. Xiang, D. Zhang, S.J. Shi, J.P. Tu, Electrochim. Acta 56 (2010) 510.
[19] Y.G. Mateyshina, N.F. Uvarov, J. Power Sources 196 (2011) 1494.
[20] M.M. Ren, Z. Zhou, Y.Z. Li, X.P. Gao, J. Yan, J. Power Sources 162 (2006) 1357.
[21] E. Kobayashi, L.S. Plashnitsa, T. Doi, S. Okada, J. Yamaki, Electrochem. Commun. 12 (2010) 894.
[22] K. Xu, Chem. Rev. 104 (2004) 4303.
[23] K. Xu, S.P. Ding, T.R. Jow, J. Electrochem. Soc. 146 (1999) A4172.
[24] Y. Li, T. Markmaitree, B.L. Lucht, J. Power Sources 196 (2011) 2251.
[25] Q.Q. Chen, J.M. Wang, Z. Tang, W.C. He, H.B. Shao, J.Q. Zhang, Electrochim. Acta 52 (2007) 5251.
[26] Y.Z. Li, Z. Zhou, M.M. Ren, X.P. Gao, J. Yan, Electrochim. Acta 51 (2006) 6498.
[27] C.W. Sun, S. Rajasekhara, Y.Z. Dong, J.B. Goodenough, ACS Appl. Mater. Interf. 3 (2011) 3772.
[28] P. Fu, Y.M. Zhao, X.N. An, Y.Z. Dong, X.M. Hou, Electrochim. Acta 52 (2007) 5281.
[29] J.J. Wang, X.L. Sun, Energy Environ. Sci. 5 (2012) 5163.
[30] H.Q. Li, H.S. Zhou, Chem. Commun. 48 (2012) 1201.
[31] L.J. Her, J.L. Hong, C.C. Chang, J. Power Sources 157 (2006) 457.
[32] K.S. Park, S.B. Schougaard, J.B. Goodenough, Adv. Mater. 19 (2007) 848.
[33] Y.G. Wang, Y.R. Wang, E. Hosono, K.X. Wang, H.S. Zhou, Angew. Chem. Int. Ed. 47 (2008) 7461.
[34] D. Lepage, C. Michot, G.X. Liang, M. Gauthier, S.B. Schougaard, Angew. Chem. Int. Ed. 50 (2011) 6884.
[35] E. Perez-Cappe, Y. Mosqueda, R. Martinez, C.R. Milian, O. Sanchez, J.A. Varela, A.H. Miranda, E. Souza, P. Aranda, E. Ruiz-Hitzky, J. Mater. Chem. 18 (2008) 3965.
[36] I. Boyano, J.A. Blazquez, I. de Meatza, M. Bengoechea, O. Miguel, H. Grande, Y. Huang, J.B. Goodenough, J. Power Sources 195 (2010) 5351.
[37] G.X. Wang, L. Yang, Y. Chen, J.Z. Wang, S. Bewlay, H.K. Liu, Electrochim. Acta 50 (2005) 4649.
[38] A.V. Murugan, T. Muraliganth, A. Manthiram, Electrochem. Commun. 10 (2008) 903.
[39] R. Jean, Chem. Rev. 92 (1992) 711.
[40] R.D. McCullough, S. Tristram-Nagle, S.P. Williams, R.D. Lowe, M. Jayaraman, J. Am. Chem. Soc. 115 (1993) 4910.
[41] K. Abe, Y. Ushigoe, H. Yoshitake, M. Yoshio, J. Power Sources 153 (2006) 328.
[42] H.-C. Wu, C.-Y. Su, D.-T. Shieh, M.-H. Yang, N.-L. Wu, Electrochem. Solid-State Lett. 9 (2006) A537.
[43] L. El Ouatani, R. Dedryvère, C. Siret, P. Biensan, S. Reynaud, P. Iratçabal, D. Gonbeau, J. Electrochem. Soc. 156 (2009) A103.
[44] R.J. Wattman, J. Bargon, A.F. Diaz, J. Phys. Chem. 87 (1983) 1459.
[45] L.Y. Xing, M. Hu, Q. Tang, J.P. Wei, X. Qin, Z. Zhou, Electrochim. Acta 59 (2012) 172.